applied sciences

IMPACT FACTOR 2.5

CITESCORE 5.3

Review

Research Prospects for the Optimization of Magneto-Optical Trap Parameters for Cold Atom Interferometers

Dongyi Li, Fangjun Qin, Rui Xu and An Li

MDPI

https://doi.org/10.3390/app14167062

applied sciences

MDPI

Review

Research Prospects for the Optimization of Magneto-Optical Trap Parameters for Cold Atom Interferometers

Dongyi Li *, Fangjun Qin, Rui Xu and An Li

School of Electrical Engineering, Naval University of Engineering, No. 717 Liberation Street, Wuhan 430033, China; haig2005@126.com (F.Q.); d22381101@nue.edu (R.X.); lian196101@126.com (A.L.)
* Correspondence: lidongyi1001@126.com; Tel./Fax: +86-15926400323

Abstract: This study examines parameter optimization for magneto-optical traps (MOTs) to increase trapping efficiency and improve cold atom interferometer performance. Operational principles of MOTs, control parameters, and performance metrics such as volume, atomic loading time, and resonance frequency are discussed. This research also reviews existing studies on the parameter optimization of MOTs, highlights challenges, and offers suggestions for future research. It proposes enhancing performance metrics, optimization techniques, and operational models to increase precision and practicality in parameter optimization for MOTs in cold atom interferometers.

Keywords: MOT; parameter optimization; laser cooling; cold atom

1. Introduction

Observing and controlling atoms at room temperature poses challenges because of their high energy states, but laser-cooled atoms serve as an advantageous experimental medium [1–7]. Cold atoms exhibit reduced motion speed and weak interaction forces, making them promising for applications in quantum optics, ultracold collisions, Bose–Einstein condensation, and precise measurements [8–11]. To manipulate cold atoms effectively in experiments, a magneto-optical trap (MOT) is utilized, which converges atoms via a combination of light and magnetic fields on the basis of this principle [12–15].

The fundamental concept of the MOT was initially introduced by Jean Dalibard and subsequently put into practice through collaboration with the research groups of Steven Chu and Pritchard [16,17]. The earliest MOT experiments involved the utilization of precooled sodium atomic beams. The original six-beam MOT setup necessitated a costly precooling apparatus and was relatively intricate [14]. In 1990, the Wieman team introduced the concept of background steam loading, simplifying the experimental procedure and facilitating the widespread adoption of MOT technology [18]. Currently, MOT technology is extensively employed in atomic physics research, encompassing various trapped atom types such as alkali metals, alkaline earth metals, inert gasses, and radioactive isotopes [19], with MOT configurations continuously evolving [20–26]. To enhance the spin polarization of cold atomic ensembles, Walker et al. proposed a spin-polarized MOT [27]. To address the limitation of cold atom density due to radiation trapping, Ketterle et al. introduced a dark MOT, which increased the atomic density within the trap center and extended the lifespan of cold atoms [28]. Various MOT schemes have been devised to streamline MOT structures, including single-beam MOTs, four-beam MOTs, and five-beam MOTs [11,29,30]. Two-dimensional MOTs, achieved by adjusting the axial beams of three-dimensional MOTs, have been widely adopted to convert trapped cold atomic ensembles into atomic beams [31–33]. Recent advancements in miniaturized cold atom sensor technology, particularly chip-level MOTs such as grating MOTs, have emerged as a prominent research focus [34,35]. These chip-level MOTs offer reduced power consumption and compact size, opening new avenues for expanding the application scope of atomic MOTs.

check for updates

Citation: Li, D.; Qin, F.; Xu, R.; Li, A. Research Prospects for the Optimization of Magneto-Optical Trap Parameters for Cold Atom Interferometers. *Appl. Sci.* **2024**, *14*, 7062. https://doi.org/10.3390/app14167062

Academic Editor: Nuno Silva

Received: 24 June 2024
Revised: 30 July 2024
Accepted: 9 August 2024
Published: 12 August 2024

In addition to altering the structure, the optimization of the MOT can also be achieved by adjusting the control parameters. This process is referred to as parameter optimization. The primary aim of parameter optimization is to evaluate how the control parameters of the MOT affect its performance index, with the goal of identifying the most effective control parameters. This optimization procedure can improve MOT performance and is crucial for the progression of MOT technology. As a vital element of cold atom interferometers, factors such as the quantity of atoms captured by the MOT, the temperature of the cold-atom ensemble, and the duration of trapping significantly affect performance. For example, in optical lattice clocks, a greater number of atoms trapped in the MOT results in an increased signal–to–noise ratio in the data collected [36]. Conversely, in atomic gravimeters, the atomic diffusion effect caused by temperature variations can reduce the contrast of interference fringes and introduce systematic errors in measurements [37]. Furthermore, in atomic gyroscopes, the quest for improved measurement accuracy and bandwidth requires enhanced atom-loading efficiency [38]. Additionally, owing to the fundamental similarities in the principles underlying different types of MOTs, parameter optimization not only enhances the trapping efficiency of existing MOTs but also has substantial implications for the advancement of novel MOT technologies.

In summary, it is crucial to optimize the parameters of the MOT to enhance its trapping effect and improve the performance of the cold atom interferometer. This paper systematically analyzes the working principle of the MOT in a cold atom interferometer, categorizes the control parameters and common performance indicators, and proposes application performance indicators relevant to the use of the MOT in a cold atom interferometer. Furthermore, the research progress and key technologies related to optimizing MOT parameters in cold atom interferometers are discussed, the main issues in parameter optimization are identified, and future development directions are outlined.

2. Analysis of the Working Principle of MOTs

2.1. Basic Structure

An MOT, also known as a scattering force trap, uses the scattering force resulting from the combined action of a magnetic field and a laser to trap atoms. Its structure diagram is depicted in Figure 1 [39,40].

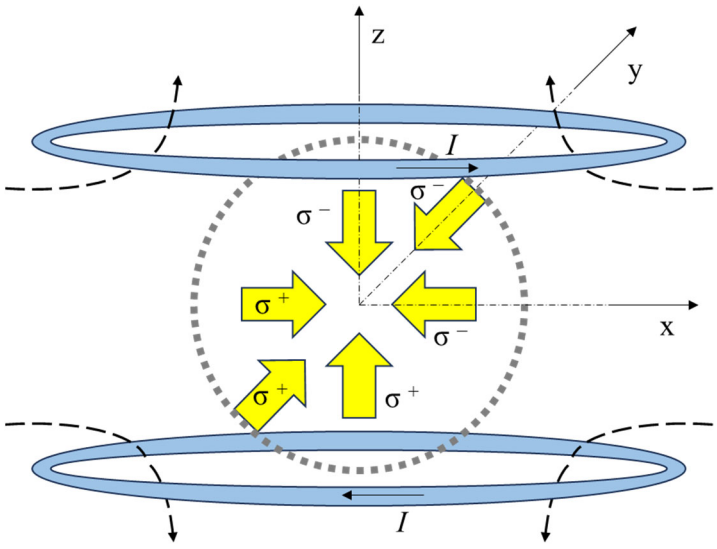

Figure 1. Diagram of a typical MOT.

The MOT consists of a vacuum chamber containing gaseous atoms (represented by gray circles), two anti-Helmholtz coils (shown as blue ellipses), and six elliptically polarized beams (indicated by yellow arrows). The coils are symmetrically distributed along the z-axis on both sides of the vacuum chamber, with the distance between the coils equal to the radius. Both coils carry the same magnitude of current I, but in opposite directions,

creating a gradient magnetic field (illustrated by black curved arrows) that starts at zero at the coordinate origin and increases linearly along the axis. The six beams are directed into the vacuum chamber along six axes, with two opposite beams polarized in opposite directions. The combination of the magnetic field and the light field from the six beams creates a potential trap that traps the atoms. The central region of the magnetic field and light field aligns with the center of the vacuum chamber, where the atoms are trapped.

2.2. Action Mechanism

Taking atoms moving along the z-axis as an example, the operational mechanism of the MOT is illustrated in Figure 2. It is assumed that the ground state has an orbital angular momentum of $S = 0$ and that the excited state has an orbital angular momentum of $S = 1$. When subjected to a gradient magnetic field, the excited state experiences Zeeman splitting, dividing into three magnetic sublevels, $m_S = -1$, $m_S = 0$, and $m_S = 1$, as depicted in Figure 2. The extent of sublevel splitting is influenced by the magnetic field strength and is linearly correlated with the position. The Zeeman shift of the magnetic sublevel decreases linearly along the z-axis for $m_S = -1$, remains constant for $m_S = 0$, and increases linearly along the z-axis for $m_S = 1$. The two beams traveling in opposite directions are polarized in opposite directions. The laser frequency ω is lower than the transition frequency of the atom, indicating negative laser detuning δ.

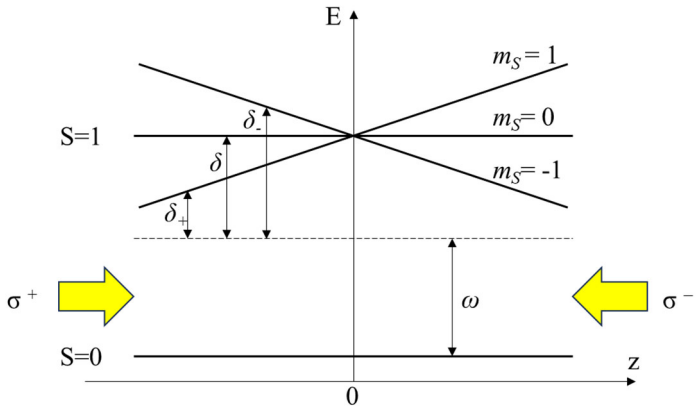

Figure 2. Schematic diagram of a one-dimensional MOT.

In the region where z > 0, the Doppler effect causes the σ^- light received by the atom to be closer to the atomic transition frequency. As a result, the atom absorbs more σ^- photons and experiences a scattering force along the z-axis. Similarly, in the region where z < 0, the atom also receives σ^+ light closer to the atomic transition frequency, leading to increased σ^+ photon absorption and a scattering force along the z-axis. The scattering force on an atom is influenced not only by its velocity but also by its position in space. As the atom moves closer to the center, the detuning value increases gradually, leading to a gradual decrease in the scattering force. This allows atoms to be trapped in the central region.

From an energy conversion standpoint, when an atom in motion is exposed to a counterpropagating laser, the perceived frequency of the laser by the atom will be slightly higher than its actual frequency ω. Upon reaching the transition frequency, the atom will undergo excited absorption, leading to a transition to the excited state upon absorbing the counterpropagating photon. However, as the atom returns to its ground state through spontaneous radiation from the excited state, the momentum of the emitted photon will not exhibit a specific direction. Through numerous iterations, the average momentum of the spontaneous radiation on the atom converges to zero, resulting in a scenario in which the atom consistently absorbs the momentum of the counterpropagating photon, leading to a continuous decrease in its velocity. By expanding this principle into three-dimensional space, a stable MOT can be established.

The preceding analysis provides a qualitative depiction of the operational mechanism of the MOT. However, the distribution of energy levels in atoms and the spatial arrangement of magnetic and light fields are intricate, necessitating the consideration of additional factors [41–44]. For example, in the context of the spontaneous radiation process of atoms, if the atom's ground state comprises multiple sublevels, subsequent to spontaneous radiation, the atoms may revert to different sublevels, impeding their involvement in the subsequent stimulated absorption. In such cases, it is necessary to add a pump laser to sustain the cooling process.

2.3. Atomic Force and Motion Analysis

The movement of a neutral atom is affected by gravity, the magnetostatic force, and the scattering force at the same time. The scattering force is approximately 1000 times greater than the combined forces of gravity and the magnetostatic force. Hence, when considering forces on atoms, only the scattering forces are typically taken into account. In the case of one dimension, the total scattering force acting on the atom can be calculated as follows [14].

$$\vec{F} = \vec{F}_+ + \vec{F}_- \tag{1}$$

$$\vec{F}_\pm = \hbar \vec{k} \frac{\Gamma}{2} \frac{\Omega^2/2}{\delta_\pm^2 + \Omega^2/2 + \Gamma^2/4} \tag{2}$$

where $\hbar = 1.0545887 \times 10^{-34}\mathrm{J} \cdot \mathrm{s}$ is the Planck constant, $\vec{k}$ is the laser wave vector, Γ is the natural line width, and Ω is the Rabi frequency. The detuning $\delta_\pm$ of the resonance transition spectrum of the laser to atoms shifts with changes in the atomic velocity and magnetic field.

$$\delta_\pm = \delta \mp \vec{k} \cdot \vec{v} \pm \mu' A x/\hbar \tag{3}$$

where $\delta = |\omega - \omega_0|$ represents the laser frequency detuning, $\vec{v}$ represents the atomic velocity, μ' represents the effective magnetic moment, A represents the axial magnetic field gradient, and x represents the coordinates of the atom on the axis.

The equation describing the motion of atoms can be formulated as follows.

$$\begin{aligned} mx'' &= \hbar k \tfrac{\Gamma}{2} \left(\tfrac{\Omega^2/2}{\delta_+^2 + \Omega^2/2 + \Gamma^2/4} \right. \\ &\quad \left. - \tfrac{\Omega^2/2}{\delta_-^2 + \Omega^2/2 + \Gamma^2/4} \right) \\ \delta_\pm &= \delta \mp \vec{k} \cdot \vec{x}' \pm \mu' A x/\hbar \\ x(0) &= x_0 \\ x'(0) &= v_0 \end{aligned} \tag{4}$$

where x_0 represents the initial position of the atom and where v_0 represents the initial velocity of the atom. The motion of atoms in the MOT can be simulated by solving the atomic motion equation via the Runge–Kutta method, given the initial velocity and position of the atoms.

Taking the ^{87}Rb atom as an example, we consider the laser intensity $I = 6\ \mathrm{mW/cm^2}$, laser radius $r = 1\mathrm{cm}$, magnetic field gradient $A = -400\ \mathrm{G/m}$, and laser detuning $\delta = -17\ \mathrm{MHz}$ in the MOT. Assuming that atoms start from the edge of the trap at different speeds, the motion velocity of each atom in the MOT varies with position, as shown in Figure 3.

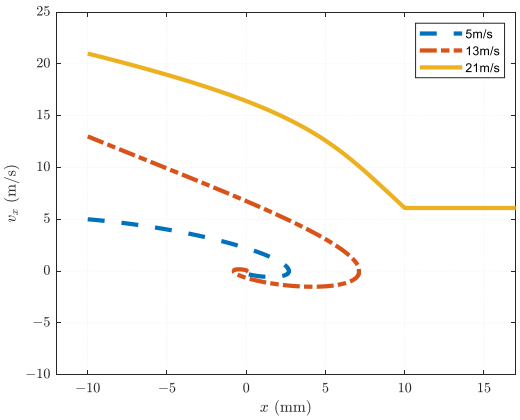

Figure 3. Atomic motion in an MOT.

In Figure 3, the area between the two black dashed lines indicates the region in which the trap has an effect. Various colored and shaped lines represent the paths of atoms with different initial velocities. Figure 3 shows that atoms starting from the edge of the trap with initial velocities of 5 m/s and 13 m/s can slow down within the trap and become trapped in the center, whereas atoms with an initial velocity of 21 m/s escape from the trap.

3. The Main Parameters and Indices of MOT

3.1. Control Parameters

MOT is created by manipulating atoms via magnetic and light fields. Its control parameters are related to these fields, as shown in Table 1.

Table 1. MOT control parameters.

Serial Number	Control Parameter Name	Unit
1	Cooling laser detuning	MHz
2	Cooling laser intensity	mW/cm^2
3	Cooling laser radius	m
4	Cooling laser polarization	—
5	Magnetic field gradient	G/cm
6	Repumping laser intensity	mW/cm^2
7	Repumping laser detuning	MHz
8	Compensated field gradient	G/cm

The detuning of the repumping laser varies depending on the type of atom used and is typically constant. The gradient of the compensated magnetic field is calibrated before measurement and remains unchanged during the measurement process. Therefore, the control parameters that frequently require adjustment mainly consist of the first six.

3.2. Conventional Performance Indices

The MOT functions to slow down and trap gaseous atoms to create cold atomic groups. As a result, the performance of the MOT is typically evaluated on the basis of the physical characteristics of the trapped atomic groups. These characteristics primarily include the number of atoms, density, temperature, and lifespan.

3.2.1. The Atomic Number

In an MOT, atoms are trapped by the trapping force but can also be hit by background atoms and escape. The number of atoms eventually trapped in the MOT is determined by the capture and escape processes. If the number of atoms is N, the rate of change is

$$\frac{dN}{dt} = R - \frac{N}{\ell} - \beta\frac{N^2}{v} \tag{5}$$

where ℓ is the atomic lifetime and R is the trapping probability. The third term on the right is caused by the double-body collision effect of atoms. This effect can be ignored when the atomic density is low. The trapping probability is related to the number of atoms entering the potential trap at a rate lower than the trapping rate v_c per unit time. It can be calculated as follows:

$$R \approx An_0 S \frac{v_c^4}{\overline{v}^3} \tag{6}$$

where A represents the correction factor, n_0 represents the background gas density, S represents the total surface area of the potential trap region, and $\overline{v}$ represents the root-mean-square velocity of the background gas atoms.

By substituting the initial conditions $N = 0$, the variation rule of the atomic number can be obtained as follows [14]:

$$\begin{aligned} N(t) &= R\ell(1 - e^{-t/\ell}) \\ &= \frac{1}{\sqrt{6}} \frac{S}{\sigma_e} v_c^4 \left(\frac{m}{2k_B T}\right)^2 (1 - e^{-t/\ell}) \end{aligned} \tag{7}$$

where σ_e is the collision cross-section of the background vapor atom colliding with the trapped atom, m is the atomic mass, and T is the cold atomic group temperature. The formula indicates that the number of atoms in the stable state is directly proportional to the fourth power of the trapping rate. This implies that the number of atoms can be estimated via the trapping rate. Moreover, the number of atoms is affected by the temperature of cold atomic groups and the lifetime of the atoms.

The atomic number is typically measured via fluorescence detection in practice.

3.2.2. Atomic Density

The atomic density in the MOT is limited primarily by two effects: the fluorescence self-trapping effect and the double-body collision effect. The fluorescence self-trapping effect creates a repulsive force between atoms in the potential trap, whereas the double-body collision effect increases the rate at which atoms escape.

The atomic density can be calculated by determining the ratio of the number of atoms to the volume of the cold atomic group. However, the distribution of atoms in the cold atomic group is not always uniform, so the atomic density obtained via this method may not be sufficiently accurate. To determine the atomic density more precisely, the weak light absorption method can be employed. This method operates on the same principles as fluorescence detection and involves measuring the laser intensity and the length of the cold atomic group to obtain the atomic density via a specific formula [45].

$$n = \frac{\ln\left(\frac{I_i}{I_o}\right)}{\sigma L(1 - 2P)} \tag{8}$$

where σ represents the resonance absorption cross-section of the atom, P represents the probability of the atom being in the excited state, I_i represents the incident laser intensity, I_o represents the outgoing laser intensity, and L represents the length of the cold atomic group.

3.2.3. Atomic Temperature

The temperature of cold atoms determines the velocity distribution of atomic groups. When atoms escape from the MOT with transverse velocity, thermal diffusion occurs, affecting subsequent test performance [37]. The temperature of the cold atom is determined by the cooling mechanism and influenced mainly by the laser intensity and the detuning.

A common method for determining the temperature of cold atomic groups is the time-of-flight method [46]. This method involves allowing the confined cold atomic group to fall freely under the influence of gravity, irradiating the falling atomic group with a detection laser beam and receiving a pulse signal containing velocity distribution information of the

cold atomic group on the photodetector. By fitting the measured velocity distribution with Formula (9), the temperature of the cold atomic group can be obtained.

$$\Delta v = 2\sqrt{\frac{2k_B T}{m}\ln 2} \tag{9}$$

where Δv is the velocity distribution width of the half-high value.

3.2.4. Atomic Lifetime

The atomic lifetime is the average duration that atoms remain in the trap, representing the average time it takes for atoms to escape from the MOT as a result of collisions. The atomic lifetime is influenced by the rate of collisions that leads to the escape of atoms per unit time.

$$\ell = \frac{1}{n_0 \sigma_e \overline{v}} \tag{10}$$

The lifetime of an atom is usually determined by monitoring the change in its atomic number during the process of atomic capture. The pattern of change in the atomic number during the capture process can be described by Formula (7), which follows an exponential trend. When the atomic number in the trap reaches a 1/e difference from its stable value, the duration of time it takes to reach this point represents the lifetime of the atom in the trap.

3.3. Application Requirement Analysis

Conventional performance indices can accurately reflect the trapping capability of the MOT for gaseous atoms and can be used to assess the performance of the MOT device. However, using MOTs to obtain cold atomic groups is just the initial step for various cold atom interferometers. To evaluate MOT performance, we should not only consider conventional performance indicators but also analyze the development requirements of various cold atom interferometers. Thus, we can propose application performance indicators that are more suitable for practical use.

The cold atom interferometer primarily includes an atomic clock, an atomic gravimeter, an atomic gravity gradiometer, and an atomic gyroscope [47–51]. The development of these devices has focused on three main aspects.

3.3.1. Miniaturization

In the early stages of development, atomic gravimeter research focused on improving sensitivity and stability, as well as exploring basic physics [52], without considering the device size. In approximately 2013, to conduct research on the detection of the equivalence principle and gravitational wave measurement, Stanford University and the Wuhan Institute of Mathematics at the Chinese Academy of Sciences developed a 10 m high fountain-type atomic gravimeter [53,54]. This device significantly increases the area of atomic interference and evolution time and improves the measurement sensitivity. In addition to basic physics research, gravity-related information also holds significant application value in inertial navigation, resource exploration, geophysics, and other fields [55,56]. In response to these application needs, the development of miniaturized and mobile atomic gravimeters has gradually become an important direction for atomic gravimeter research. Various experiments have been conducted on elevator measurements, vehicle measurements, ship measurements, and airborne measurements, and the adaptability of atomic gravimeters in complex environments has become increasingly important.

The miniaturization of other devices is also necessary. For example, small atomic clocks can offer highly precise time references for mobile devices to ensure accurate data transmission [57,58]. In the military sector, miniaturized atomic gyroscopes can enhance the performance of inertial navigation systems, improving the navigation and attitude control accuracy of space vehicles [59–61]. Furthermore, miniaturized atomic gravity gradiometers can provide gravity compensation data for inertial navigation devices, reducing the impact

of vertical line deviation and supporting the high-precision long-endurance navigation of underwater carriers, such as submarines [62,63].

3.3.2. Reduce Measurement Noise

In high-precision measuring instruments, environmental noise can significantly impact device stability and reliability, as well as measurement resolution. The noise in an atomic gravimeter comprises Raman laser phase noise, Raman laser intensity noise, vibration noise, detection noise, and quantum projection noise. Among these methods, the use of mirror vibration noise poses the greatest challenge [64,65]. A gravity gradiometer employs a differential measurement mechanism to effectively suppress Raman laser phase noise, Raman laser intensity noise, and mirror vibration noise, but it cannot suppress Raman laser frequency noise and magnetic field noise [66–68]. In an atomic clock, mechanical vibration can introduce noise into the laser and atomic system, leading to inaccuracies in the frequency locking of the spectral line and reduced output signal stability [58]. Similarly, in a continuous cold atomic beam interference gyroscope, interference fringes may be affected by atomic beam flux fluctuations, Raman optical power jitter, Raman optical phase jitter, and other factors, resulting in measurement noise [69].

3.3.3. Increasing the Measurement Bandwidth

When a gravimeter from a research team is used as an example, please refer to Figure 4 [70] for the timing diagram of the gravity measurement. The gravity measurements should be conducted from left to right. The figure indicates the time required for each stage and the total time (T_a).

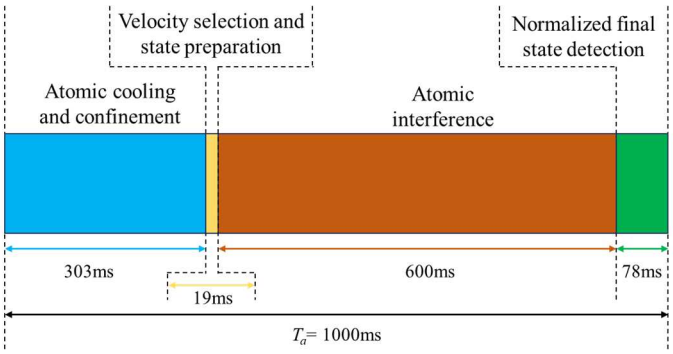

Figure 4. Atomic gravimeter measurement sequence diagram.

In Figure 4, it is evident that only 60% of the total time is dedicated to atomic interference. Additionally, there is a substantial measurement dead zone in each cycle of the atomic gravimeter. This dead zone arises from the time spent on atomic cooling and confinement, speed selection, state preparation, normalized final state detection, and other stages. The existence of this dead zone reduces the measurement efficiency, limits the improvement of the measurement bandwidth, and makes eliminating some resonance noise challenging. As the use of atomic gravimeter dynamic measurements continues to progress, the issue of measurement bandwidth has been increasingly discussed [71].

In atomic gyroscopes, while the development of nuclear magnetic resonance gyroscopes has matured, the theoretical accuracy of atomic interference gyroscopes has increased, making them more suitable for applications in strategic weapons and equipment. However, atomic interference gyroscopes currently face challenges related to their narrow measurement bandwidth and limited range, which restrict their application range [72].

3.4. Application Performance Indices

To fulfill the application requirements of the aforementioned devices, three additional application performance indices should be incorporated to enhance the MOT evaluation system.

3.4.1. Volume

A typical structural diagram of an atomic gravimeter, which includes a measuring probe and a vibration isolation platform, is shown in Figure 5 [73]. The measuring probe is divided into three regions: the preparation region, the interference region, and the detection region. In the preparation region, six beams of a cooling laser are used to trap the atoms. The interference region requires a Raman laser and its reflected laser to change the atomic state.

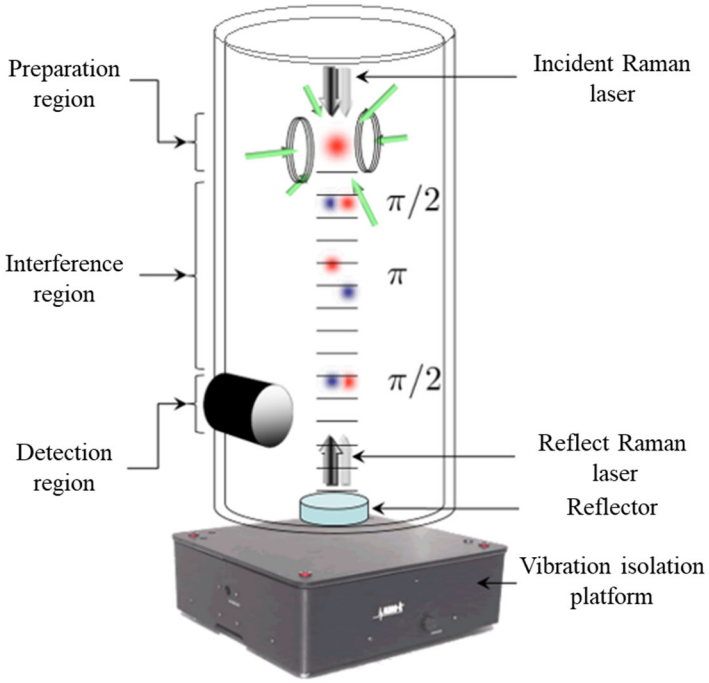

Figure 5. Atomic gravimeter structure diagram.

Figure 5 clearly shows that trapping atomic groups in the vacuum region via an MOT requires numerous beams and a complex spatial structure. These factors are crucial when considering the miniaturization of such devices. Therefore, the volume of the MOT serves as the primary performance index for devices.

Efforts have been made to reduce the size of the MOT and enhance device integration. Research on pyramids, grating MOTs, and chip MOTs has been conducted [74–76], and these methods have gradually been implemented in practical devices [77,78].

3.4.2. Resonant Frequency

The trapping process of an MOT is influenced by vibration and noise. Taking a one-dimensional MOT as an example, the variations in the atomic number under different vibration frequencies and laser intensities are illustrated in Figure 6 [79].

Figure 6 clearly shows that the MOT has a resonant frequency of approximately 500 Hz. When the vibration frequency closely matches the resonant frequency, the number of captured atoms is minimized. Conversely, when the vibration frequency deviates from the resonant frequency, the number of captured atoms increases. The resonant frequency is an important indicator for evaluating the impact of vibration and noise on the atomic cooling and trapping process, thus improving the overall device performance. Various methods for measuring the MOT's resonance frequency include transient oscillation, harmonic oscillation, parametric resonance, and cooling laser intensity modulation [79].

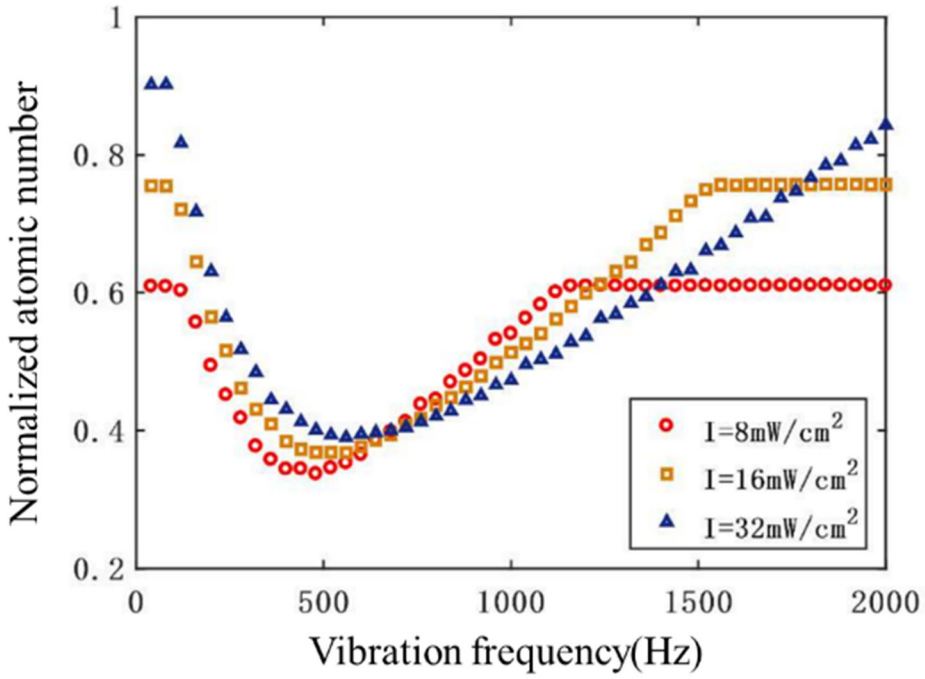

Figure 6. The number of atoms at various vibration frequencies and laser intensities.

3.4.3. Atomic Loading Time

In Figure 4, the time taken to load the atoms makes up 76% of the measured dead zone and is a major part of the dead zone time. Additionally, the process of loading the atoms is only a preparation stage and does not collect any useful information. By reducing the time it takes to load the atoms, we can shorten the measurement cycle, increase the data rate of the measurement process, and leave more time for the more important stage of collecting information. Therefore, it is important to consider the time it takes to load the atoms when evaluating the performance of the MOT and to have a more thorough discussion about it.

Using the MOT in the atomic gravimeter developed by Zhejiang University as an example, Figure 7 shows how the number of atoms changes as the loading time increases during operation [77]. Initially, the number of atoms quickly increases, but then the growth rate decreases after a certain point is reached.

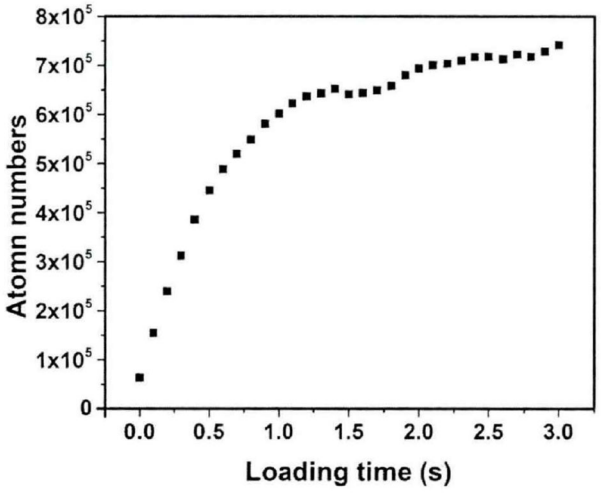

Figure 7. Atom-loading process in the MOT.

The time required for the saturation of the number of atoms, which is known as the atomic loading time, as shown in Figure 7, is 2 s.

Based on the discussion in this section, the performance indicators of the MOT are shown in Table 2.

Table 2. MOT performance indices.

Serial Number	Performance Indicator Name	Unit
1	Atomic number	-
2	Atomic density	-
3	Atomic temperature	K
4	Atomic lifetime	s
5	Volume	m^3
6	Resonant frequency	Hz
7	Atomic loading time	s

4. Prospects for Research on the Optimization of MOT Parameters

4.1. Research Progress

The parameter optimization of the MOT involves a thorough analysis of how the MOT operates. This analysis evaluates how each control parameter affects the trapping performance. The optimal combination of control parameters is then applied to the actual device to improve the trapping performance of the MOT. Currently, there is limited research on optimizing MOT parameters for cold atom interferometers. The existing studies on parameter optimization are presented in chronological order. The molecular MOTs operate similarly to the atomic MOTs and are discussed in conjunction.

In 2006, Jiang Kaijun analyzed the variation trend of the atomic number with cooling laser intensity, cooling laser detuning, repumping laser intensity, and magnetic field gradient for Rb atomic MOTs. Some of the test results were in agreement with the results predicted by the two-level system model, which initiated the preliminary exploration of the parameter optimization of MOTs [80].

In 2016, Gou Wei analyzed the one-dimensional atomic motion equation in the MOT of mercury atoms. Gou Wei numerically simulated the relationships between the atomic number in a three-dimensional MOT and the laser intensity, laser detuning, and magnetic field gradient via the random number method, thus further improving the accuracy of the model [36].

From 2017 to 2019, Wu Liming analyzed the effects of pushing a laser, magnetic field gradient, geomagnetic field, cooling laser power, and cooling laser detuning on the steady-state atomic number with the help of a specific test device. Wu Liming gave the influence rule of each parameter and finally increased the steady-state atomic number trapped by the MOT of Rb atoms by an order of magnitude, achieving a good optimization effect [81].

In 2018, A.D. Terranter introduced an artificial neural network into the control feedback loop to complete parameter optimization in the actual MOT system. The optimized system performance was better than that of the most well-known solutions and generated a higher optical density [82].

In 2021, Liu Qian proposed a multiparameter autonomous optimization system based on an artificial neural network and applied it to the atomic motion model of MOT constructed via the Monte Carlo simulation method. Four parameters, including the cooling laser power, cooling laser detuning, magnetic field gradient, and axial velocity of the atomic beam from the two-dimensional MOT, were optimized with the atomic number as the ultimate goal. Reliable and stable optimum test results were obtained [83].

Additionally, in 2021, S Xu et al. from Leibniz University of Hanover, Germany, focused on the trapping rate of CaF molecular MOT as the main goal. They comprehensively considered a parameter set composed of 14 parameters in the polarization state of the cooled laser, the intensity of the cooled laser, the cooling laser detuning, the magnetic field gradient, and the cooling laser radius under the condition of a certain total laser power. The maximum trapping velocity and the corresponding parameter combination were found via

the Bayes optimization tool. There is also a certain logarithmic relationship between the trapping rate and the laser power [84].

In 2023, Li Jiaxin used the Runge–Kutta method to solve the equation of atomic motion and simulated the working process of a two-dimensional MOT via the Monte Carlo method. Li Jiaxin analyzed the variation in the atomic beam flux with the magnetic field gradient, cooling laser detuning, laser intensity, and other parameters and proposed an optimal parameter combination to increase the atomic beam flux [85].

Additionally, in 2023, Chen Lang proposed a cold atom multiparameter autonomous real-time optimization experimental scheme based on the Bayesian optimization method. This scheme forms an autonomously optimized closed-loop system through cost function construction, control program programming, and Bayesian algorithm optimization. After 30 min of real-time optimization, the number of trapped atoms effectively increased, and the atomic group temperature decreased [86].

4.2. Several Key Technologies

To ensure effective parameter optimization, two factors should be focused on:

1. Complete MOT working model: The working model is crucial for parameter optimization and serves as a key tool for testing the optimization effectiveness. It should accurately represent the forces and motion of atoms in the MOT. The most effective working model is the actual MOT device, as using the real device for parameter optimization yields the most reliable results. However, since the actual MOT is typically coupled with other devices, it is impractical to repeatedly switch the entire testing setup and adjust the control parameters to analyze the trapping performance of the MOT separately. Therefore, the actual device can be used for optimization work only when the optimized performance indicators can be directly detected. Another approach is to create a numerical model of the MOT on the basis of the actual device to simulate atomic motion within the MOT. This method is not limited by the device and allows for easier adjustment of the control parameters with strong repeatability, but it requires ensuring the accuracy of the model. Currently, the working models used in parameter optimization research include practical devices and numerical models.

2. Efficient multiparameter optimization method: The optimization method is a crucial tool for parameter optimization and directly impacts its efficiency. The more targets and control parameters there are to be optimized and adjusted, the higher the performance requirements for the optimization algorithm. Currently, the dominant optimization method used in optimizing MOT parameters is the control variable method. This method involves analyzing the influence of each control parameter on the optimization objective based on a known model and then determining the optimal value for each control parameter to form the optimal control parameter set. In recent years, advancements in machine learning, artificial intelligence, and other technologies have led to the development of various intelligent algorithms that demonstrate strong computational efficiency and data accuracy in addressing optimization problems, resulting in significant achievements [87].

The research outputs of each team, including the working models, optimization methods, and performance indicators, are summarized in Table 3.

Table 3. Review of the research progress on parameter optimization.

Years	Research Team Member	Working Model	Optimization Method	Performance Index
2006	Jiang Kaijun	Real system, two-level model	Control variable method	Atomic number
2016	Gou Wei	Random number method simulation based on motion equation	Control variable method	Atomic number
2017–2019	Wu Liming	Actual system	Control variable method	Atomic number
2018	A.D. Tranter	Actual system	Artificial neural network	Optical density
2021	Liu Qian	Monte Carlo simulation based on motion equation	Artificial neural network	Atomic number

Table 3. *Cont.*

Years	Research Team Member	Working Model	Optimization Method	Performance Index
2021	S Xu	Rate equation model	Bayesian optimization	Trapping rate
2023	Li Jiaxin	Monte Carlo simulation based on motion equation	Control variable method	Atomic beam flux
2023	Chen Lang	Actual system	Bayesian optimization	Atomic group fluorescence

4.3. Some Suggestions for Parameter Optimization Research

Parameter optimization is crucial for improving the performance of MOTs and expanding their applications. Some research has already been conducted in this area. Despite the complex structure of MOTs, many research teams have successfully applied parameter optimization in real systems and achieved excellent results. Numerical models have also been advanced to simulate more complex atomic motion states. Furthermore, the variety of optimization methods is increasing, leading to improved computational efficiency and accuracy. Research on optimizing atomic MOT parameters can be further improved in the following areas.

(1) It is important to use multiple performance indicators rather than just focusing on the number of atoms to optimize the MOT. Table 3 shows that the capture velocity, atomic beam flux, and atomic group fluorescence are strongly correlated with the number of atoms. Many research teams, with the exception of A.D. Terranter's team, primarily used the number of atoms as the ultimate performance indicator for parameter optimization. However, as shown in Table 2, several indicators are used to measure the trapping performance of the MOT, including the temperature, density, and lifetime of the atomic group, as well as the resonance frequency of the trap and the atomic loading time. These performance indicators are equally important for evaluating the performance of MOTs and should be thoroughly studied.

(2) Enhancing the research of optimization methods is important. Currently used methods include the control variable method, artificial neural network, and Bayesian optimization. While the control variable method's principle is simple, it takes a long time and requires that each parameter independently affects the result [88]. However, many control parameters of the MOT can interact with each other [83]. Artificial neural networks and Bayesian optimization address the limitations of the control variable method and can determine the optimal control parameter combination more quickly and accurately. The number of applied optimization methods is relatively small at present, and there is a lack of horizontal comparisons between various methods. Therefore, it is necessary to continue exploring optimization methods.

(3) Use reference indicators that are easy to measure instead of performance indicators. Many performance indices in MOTs cannot be measured in real time, which presents challenges for parameter optimization. The number of atoms, for example, usually requires artificially finding complete groups of atoms in the image to be accurately measured. However, parameter optimization requires multiple measurements of the number of atoms and feedback under various complex conditions, and it is obvious that other methods are needed to complete the measurement. To overcome this difficulty, Chen Lang used the fluorescence of atomic groups in a fixed region instead of the number of atoms as a performance index to carry out research and ultimately achieved the same effect of increasing the number of atoms [86]. For the other performance indicators listed in Table 2, if there are difficulties in parameter optimization, appropriate reference indicators should also be selected to replace them.

(4) Build more accurate numerical models. The working models of atomic MOT parameter optimization include practical systems and numerical models. Compared with the real system, the numerical model has no actual structure, so it is easier to adjust and obtain the control parameters and performance indicators, and it is easier to combine with various optimization methods. However, the accuracy of numerical models is difficult

to guarantee. Although the MOT principle has been proposed for more than 30 years, owing to the complexity of cold atom theory and the optical magnetic principle, it is still difficult to reproduce the atomic motion process that can guide practical applications through numerical simulation [89–91]. In the study of atomic MOT parameter optimization, although the team establishing the numerical model has achieved the optimization of various performance indicators, comparative analysis with the actual system is lacking, and the accuracy of the numerical model cannot be guaranteed. To fully exploit the advantages of numerical models in parameter optimization, we should continue to promote the comparison and verification of numerical models with actual systems and gradually build more accurate numerical models on this basis.

5. Summary and Prospects

With the further development of MOT research, an increasing number of new structures and functions of MOTs have been put into use, which greatly enriches the application field of MOTs. Improving the trapping effect of atoms in cold atom interferometers by means of parameter optimization is also an important development direction for atomic MOT. This paper introduces the working principle of the MOT of a cold atom interferometer. In addition to the conventional performance indices, three application performance indices are proposed, namely the volume, resonant frequency, and atomic loading time, which enrich the performance evaluation system of the MOT. Additionally, the development and research status of the parameter optimization of the MOT were reviewed, the main problems existing in the current parameter optimization research were discussed, and some development suggestions are given. In the future, the optimization of atomic MOT parameters needs to involve more adequate analysis and research on the selection of performance indicators and the application of intelligent algorithms, and more diverse performance indicators should be considered to comprehensively improve the trapping performance of MOTs while introducing more kinds of intelligent algorithms and carrying out comparative analysis. The working model is the main body of the parameter optimization of the atomic MOT. When the actual system is used as the working model, the reference index that can be measured automatically in real time should be selected to represent the performance index, which can promote the integration between the actual system and the optimization method and is more conducive to parameter optimization. When the numerical model is used as the working model, it is necessary to compare and verify the actual system as soon as possible to continuously improve the accuracy of the numerical model.

Author Contributions: Investigation, R.X.; writing—original draft preparation, D.L.; writing—review and editing, F.Q.; funding acquisition, A.L. All authors have read and agreed to the published version of the manuscript.

Funding: This research was funded by the National Natural Science Foundation of China (Grant. No. 42274013).

Informed Consent Statement: Not applicable.

Data Availability Statement: Not applicable.

Conflicts of Interest: The authors declare no conflicts of interest.

References

1. Höschele, J.; Buob, S.; Rubio-Abadal, A.; Makhalov, V.; Tarruell, L. Atom-number enhancement by shielding atoms from losses in strontium magneto-optical traps. *Phys. Rev. Appl.* **2023**, *19*, 064011. [CrossRef]
2. Lett, P.D.; Watts, R.N.; Westbrook, C.I.; Phillips, W.D.; Gould, P.L.; Metcalf, H.J. Observation of atoms laser cooled below the Doppler limit. *Phys. Rev. Lett.* **1988**, *61*, 169. [CrossRef] [PubMed]
3. Ali, D.B.; Badr, T.; Brézillon, T.; Dubessy, R.; Perrin, H.; Perrin, A.J. Detailed study of a transverse field Zeeman slower. *Phys. B At. Mol. Opt. Phys.* **2017**, *50*, 055008. [CrossRef]
4. Tarbutt, M.R.; Steimle, T.C. Modeling magneto-optical trapping of CaF molecules. *Phys. Rev. A* **2015**, *92*, 053401. [CrossRef]
5. Zhang, S.Z.; Sun, W.J.; Dong, M.; Wu, H.B.; Li, R.; Zhang, X.J.; Zhang, J.Y.; Cheng, Y.J. Vacuum pressure measurement based on ^{6}Li cold atoms in a magneto-optical trap. *Acta Phys. Sin.* **2022**, *71*, 145–152.

6. Lü, D.S.; Ren, W.; Sun, Y.; Li, T.; Qu, Q.Z.; Wang, B.; Li, L.; Zhao, J.B.; Zhao, X.; Ji, J.W.; et al. Characterization of Laser Cooling in Orbital Microgravity via Long-term Operations in a Space Lab. *Natl. Sci. Rev.* **2023**, *10*, nwac180. [CrossRef] [PubMed]
7. Wang, J.Y.; Liu, B.; Diao, W.T.; Jin, G.; He, J.; Wang, J.M. Optimization of the light-induced-fluorescence signals of single atoms and efficient loading of single atoms into a magneto-optical trap. *Acta Phys. Sin.* **2014**, *63*, 138–142.
8. Anderson, M.H.; Ensher, J.R.; Matthews, M.R.; Wieman, C.E.; Cornell, E.A. Observation of Bose-Einstein condensation in a dilute atomic vapor. *Science* **1995**, *269*, 198–201. [CrossRef] [PubMed]
9. Wineland, D.J.; Itano, W.M. Laser cooling of atoms. *Phys. Rev. A* **1979**, *20*, 1521. [CrossRef]
10. Cataliotti, F.S.; Burger, S.; Fort, C.; Maddaloni, P.; Minardi, F.; Trombettoni, A.; Smerzi, A.; Inguscio, M. Josephson junction arrays with Bose-Einstein condensates. *Science* **2001**, *293*, 843–846. [CrossRef]
11. Wu, X.; Pagel, Z.; Malek, B.S.; Nguyen, T.H.; Zi, F.; Scheirer, D.S.; Müller, H. Gravity surveys using a mobile atom interferometer. *Sci. Adv.* **2019**, *5*, eaax0800. [CrossRef] [PubMed]
12. Luo, K.; Pan, X.Q.; Zhou, Q.; Lu, J.F. A Combinative Double-Well Optical Trap for Two-Species Cold Atoms. *Jiangxi Sci.* **2011**, *29*, 694–697+728.
13. Huang, X.M.; Liu, X.L. The Field Structures of Some Typical Magnetostatic Traps. *J. Xiangtan Univ. (Nat. Sci. Ed.)* **2006**, *28*, 58–63.
14. Wang, Y.Q. *Laser Cooling and Trapping of Atoms*; Science Press: Beijing, China, 2007.
15. Gaudesius, M.; Zhang, Y.C.; Pohl, T.; Kaiser, R.; Labeyrie, G. Three-dimensional simulations of spatiotemporal instabilities in a magneto-optical trap. *Phys. Rev. A* **2022**, *105*, 013112. [CrossRef]
16. Raab, E.L.; Prentiss, M.; Cable, A.; Chu, S.; Pritchard, D.E. Trapping of neutral sodium atoms with radiation pressure. *Phys. Rev. Lett.* **1987**, *59*, 2631. [CrossRef]
17. Chu, S. The manipulation of neutral particles. *Rev. Mod. Phys.* **1998**, *70*, 685. [CrossRef]
18. Monroe, C.; Swann, W.; Robinson, H.; Wieman, C. Very cold trapped atoms in a vapor cell. *Phys. Rev. Lett.* **1990**, *65*, 1571. [CrossRef]
19. Cohen-Tannoudji, C.; Dupont-Roc, J. Experimental study of Zeeman light shifts in weak magnetic fields. *Phys. Rev. A* **1972**, *5*, 968. [CrossRef]
20. Xu, S.; Li, R.; Zhai, Y.; Xia, Y.; Siercke, M.; Ospelkaus, S. Blue-detuned molecular magneto-optical trap schemes based on bayesian optimization. *Phys. Rev. A* **2023**, *108*, 033102. [CrossRef]
21. Burau, J.J.; Aggarwal, P.; Mehling, K.; Ye, J. Blue-Detuned Magneto-Optical Trap of Molecules. *Phys. Rev. Lett.* **2023**, *130*, 193401. [CrossRef]
22. Shimizu, F.; Shimizu, K.; Takuma, H. Four-beam laser trap of neutral atoms. *Opt. Lett.* **1991**, *16*, 339–341. [CrossRef] [PubMed]
23. Barker, D.S.; Norrgard, E.B.; Klimov, N.N.; Fedchak, J.A.; Scherschligt, J.; Eckel, S. Single-beam Zeeman slower and magneto-optical trap using a nanofabricated grating. *Phys. Rev. Appl.* **2019**, *11*, 064023. [CrossRef] [PubMed]
24. Hyodo, M.; Nakayama, K.; Watanabe, M.; Ohmukai, R. Mirror magneto-optical trap exploiting hexapole-compensated magnetic field. *Phys. Rev. A* **2007**, *76*, 013419. [CrossRef]
25. Xu, S.; Xia, M.; Gu, R.; Yin, Y.; Xu, L.; Xia, Y.; Yin, J. Three-dimensional modeling of magneto-optical trapping of MgF molecules with multilevel rate equations. *Phys. Rev. A* **2019**, *99*, 033408. [CrossRef]
26. Williams, H.J.; Truppe, S.; Hambach, M.; Caldwell, L.; Fitch, N.J.; Hinds, E.A.; Sauer, B.E.; Tarbutt, M.R. Characteristics of a magneto-optical trap of molecules. *New J. Phys.* **2017**, *19*, 113035. [CrossRef]
27. Walker, T.; Feng, P.; Hoffmann, D.; Williamson, R.S. Spin-polarized spontaneous-force atom trap. *Phys. Rev. Lett.* **1992**, *69*, 2168. [CrossRef]
28. Ketterle, W.; Davis, K.B.; Joffe, A.; Martin, A.; Pritchard, D.E. High densities of cold atoms in a dark spontaneous-force optical trap. *Phys. Rev. Lett.* **1993**, *70*, 2253. [CrossRef]
29. Ménoret, V.; Vermeulen, P.; Le Moigne, N.; Bonvalot, S.; Bouyer, P.; Landragin, A.; Desruelle, B. Gravity measurements below 10−9 g with a transportable absolute quantum gravimeter. *Sci Rep.* **2018**, *8*, 12300. [CrossRef]
30. Wu, X.; Weiner, S.; Pagel, Z.; Malek, B.S.; Muller, H. Mobile Quantum Gravimeter with a Novel Pyramidal Magneto-Optical Trap. In *CLEO: QELS_Fundamental Science*; JW2C.5; Optica Publishing Group: Washington, DC, USA, 2020.
31. Wu, C.J.; Ruan, J.; Chen, J.; Zhang, H.; Zhang, S.G. A two-dimensional magneto-optical trap for a cesium fountain clock. *Acta Phys. Sin.* **2013**, *62*, 128–132.
32. Ruan, J.; Wu, C.J.; Liu, D.D.; Ma, J.; Zhang, S.G. Numerical simulation of generation of the Cs atom beam by two-dimensional magneto-optical trap. *J. At. Mol. Phys.* **2012**, *29*, 783–788.
33. Barbiero, M.; Tarallo, M.G.; Calonico, D.; Levi, F.; Lamporesi, G.; Ferrari, G. Sideband-Enhanced Cold Atomic Source for Optical Clocks. *Phys. Rev. Appl.* **2020**, *13*, 014013. [CrossRef]
34. Jongmin, L.; Roger, D.; Justin, C.; Randy, R.R.; Aaron, I.; Daniel, P.G.; David, B.; Kyle, H.F.; William, K.; Patrick, S.F.; et al. A compact cold-atom interferometer with a high data-rate grating magneto-optical trap and a photonic-integrated-circuit-compatible laser system. *Nat. Commun.* **2022**, *13*, 5131.
35. Lee, J.; Grover, J.A.; Orozco, L.A.; Rolston, S.L. Sub-Doppler cooling of neutral atoms in a grating magneto-optical trap. *JOSA B* **2013**, *30*, 2869–2874. [CrossRef]
36. Gou, W.; Liu, K.K.; Fu, X.H.; Zhao, R.C.; Sun, J.F.; Xu, Z. Optimization of the loading rate of magneto-optical trap for neutral mercury atom. *Acta Phys. Sin.* **2016**, *65*, 7–13. [CrossRef]

37. Louchet-Chauvet, A.; Farah, T.; Bodart, Q.; Clairon, A.; Landragin, A.; Merlet, S.; Dos Santos, F.P. The influence of transverse motion within an atomic gravimeter. *New J. Phys.* **2011**, *13*, 065025. [CrossRef]
38. Li, R.B.; Yao, Z.W.; Lu, S.B.; Jiang, M.; Li, S.K.; Wang, J.; Zhan, M.S. Precision Measurement and Applieations with Atom Interference Gyroscopes. *Navig. Position. Timing* **2021**, *8*, 8–17.
39. Gaudesius, M. Self-Oscillating Clouds in Magneto-Optical Traps. Ph.D. Thesis, Université Côte d'Azur, Nice, France, 2021.
40. Krzysztof, K.; Xuan, K.D.; Małgorzata, G.; Huy, B.N.; Jerzy, S. Magneto-optical trap: Fundamentals and realization. *CMST* **2010**, *2*, 115–129. [CrossRef]
41. Tarbutt, M.R. Magneto-optical trapping forces for atoms and molecules with complex level structures. *New J. Phys.* **2015**, *17*, 015007. [CrossRef]
42. Jarvis, K.N.; Sauer, B.E.; Tarbutt, M.R. Characteristics of unconventional Rb magneto-optical traps. *Phys. Rev. A* **2018**, *98*, 043432. [CrossRef]
43. Baum, L.; Vilas, N.B.; Hallas, C.; Augenbraun, B.L.; Raval, S.; Mitra, D.; Doyle, J.M. 1D Magneto-Optical Trap of Polyatomic Molecules. *Phys. Rev. Lett.* **2020**, *124*, 133201. [CrossRef]
44. Jarvis, K.N.; Devlin, J.A.; Wall, T.E.; Sauer, B.E.; Tarbutt, M.R. Blue-Detuned Magneto-Optical Trap. *Phys. Rev. Lett.* **2018**, *120*, 083201. [CrossRef] [PubMed]
45. Li, Y.M.; Chen, X.Z.; Wang, Q.J.; Wang, Y.Q. Motion of cesium atoms in the one-dimensional magneto-optical trap. *Acta Phys. Sin. (Oversea Ed.)* **1995**, *4*, 727.
46. Brzozowski, T.M.; Maczynska, M.; Zawada, M.; Zachorowski, J.; Gawlik, W. Time-of-flight measurement of the temperature of cold atoms for short trap–probe beam distances. *J. Opt. B Quantum Semiclassical Opt.* **2002**, *4*, 62. [CrossRef]
47. Vovrosh, J.; Wilkinson, K.; Hedges, S.; McGovern, K.; Hayati, F.; Carson, C.; Selyem, A.; Winch, J.; Stray, B.; Earl, L.; et al. Magneto-optical trapping in a near-suface borehole. *PLoS ONE* **2023**, *18*, e0288353. [CrossRef] [PubMed]
48. Mao, Y.; Sun, Z.M.; Jia, X.L.; Song, X.Y.; Jiang, Q.X. Analyzing the current situation of quantum navigation technology system. *GNSS World China* **2023**, *48*, 19–23.
49. Wang, T.; Lu, X.T.; Zhang, X.F. Research Advances in Optical Lattice Atomic Clocks. *Low Temp. Phys. Lett.* **2022**, *44*, 385–395.
50. Chen, X.Z.; He, X.; Yuan, Z.C.; Xie, W.B.; Chen, N.; Xiong, Z.Z.; Fang, S.W.; Wang, Q.; Qi, X.H. Development of compact optically pumped hot and cold cesium beam atomic clocks in Peking University. *J. Time Freq.* **2022**, *45*, 104–109.
51. Ren, L.C.; Zhou, L.; Li, R.B.; Liu, M.; Wang, J.; Zhan, M.S. Dependence of sensitivity of atom interferometer gravimeters on the Raman laser pulse sequences. *Acta Phys. Sin.* **2009**, *58*, 8230–8235.
52. Deng, X.B.; Xu, W.J.; Cheng, Y.; Zhang, J.Y.; Hu, Z.K.; Zhou, M.K. Miniaturized Atom Gravimeter and Its Application. *Navig. Control* **2022**, *21*, 66–79.
53. Sugarbaker, A. Atom interferometry in a 10 m fountain. Ph.D. Thesis, Stanford University, San Francisco, CA, USA, 2014.
54. Zhou, L.; Xiong, Z.Y.; Yang, W.; Tang, B.; Peng, W.C.; Hao, K.; Li, R.B.; Liu, M.; Wang, J.; Zhan, M.S. Development of an atom gravimeter and status of the 10-meter atominterferometer for precision gravity measurement. *Gen. Relativ. Gravit.* **2011**, *43*, 1931–1942.
55. Fu, Z.; Wang, Q.; Wang, Z.; Wu, B.; Cheng, B.; Lin, Q. Participation in the absolute gravity comparison with a compact cold atom gravimeter. *Chin. Opt. Lett.* **2019**, *17*, 011204.
56. Zhang, X.; Yan, S.H.; Zhu, L.X.; Jia, A.A.; Wang, Y.N.; Li, Q.X.; Zhang, H.K.; Yang, J. Research Status of Cold Atom Interferometric Quantum Sensors in Applications of Navigation. In Proceedings of the 10th Annual China Satellite Navigation Conference, Beijing, China, 22–25 May 2019.
57. Le Targat, R.; Lorini, L.; Le Coq, Y.; Zawada, M.; Guéna, J.; Abgrall, M.; Gurov, M.; Rosenbusch, P.; Rovera, D.G.; Nagórny, B.; et al. Experimental realization of an optical second with strontium lattice clocks. *Nat. Commun.* **2013**, *4*, 2109. [CrossRef] [PubMed]
58. Yang, Q.H.; Pan, D.; Chen, J.B. Research Progress of Chip-Scale Atomic Clocks. *Vac. Electron.* **2023**, *1*, 1–11. [CrossRef]
59. Chen, H.H.; Yao, Z.W.; Lu, Z.X.; Mao, Y.F.; Li, R.B.; Wang, J.; Zhan, M.S. Transportable High-precision Atom-interferometer Gyroscope. *Navig. Control* **2022**, *21*, 42–50+9.
60. Wang, W.; Wang, X.F.; Ma, J.L.; Yang, Y.B.; Chen, X.Z. Key Technolegy and Development of Atom Interferometric Gyroscope. *Navig. Control* **2011**, *10*, 55–60+46.
61. Luo, M.R.; Li, S.L.; Huang, Y.M.; Zhang, C.; Wu, Z.C.; Liu, H. Review and Prospect of Atomic Gyroscope Development. *Meas. Control Technol.* **2023**, *42*, 1–10. [CrossRef]
62. Wei, X.T. Summarize of Gravity Gradient Research Progress with Atom Interferometer. *Opt. Optoelectron. Technol.* **2017**, *15*, 99–104.
63. Xu, W.H.; Lu, W.; Zhong, J.Q.; Wang, J.; Zhan, M.S. Development Status and Analysis of Gravity Gradiometer Based on Atom Interferometer. *Navig. Control* **2022**, *21*, 80–90+65.
64. Tang, B.; Zhou, L.; Xiong, Z.Y.; Wang, J. A programmable broadband low frequency active vibration isolation system for atom interferometry. *Rev. Sci. Instrum.* **2014**, *85*, 093109. [CrossRef]
65. Zhang, N.; Hu, Q.; Wang, Q.; Ji, Q.; Zhao, W.; Wei, R.; Wang, Y. Michelson laser interferometer-based vibration noise contribution measurement method for cold atom interferometry gravimeter. *Chin. Phys. B* **2020**, *29*, 070601. [CrossRef]
66. Foster, G.T.; Fixler, J.B.; McGuirk, J.M.; Kasevich, M.A. Method of phase extraction between coupled atom interferometers using ellipse-specific fitting. *Opt. Lett.* **2002**, *27*, 951–953. [CrossRef] [PubMed]

67. Yang, G.D.; Weng, K.X.; Wu, B.; Cheng, B.; Lin, Q. Research Progress of Quantum Gravity Gradiometer. *Navig. Position. Timing* **2021**, *8*, 18–29.
68. Song, H.W. Development Status and Tendency of Cold-Atom Gravity Gradiometer. *Opt. Optoelectron. Technol.* **2023**, *21*, 1–14.
69. Wang, A.Q.; Meng, Z.X.; Li, Y.Y.; Xue, H.B.; Feng, Y.Y. Research Progress in a Continuous Cold Atomic Beam Interferometer Gyroscope. *Navig. Position. Timing* **2017**, *4*, 77–84.
70. Hu, Z.K.; Sun, B.L.; Duan, X.C.; Zhou, M.K.; Chen, L.L.; Zhan, S.; Zhang, Q.Z.; Luo, J. Demonstration of an ultrahigh-sensitivity atom-interferometry absolute gravimeter. *Phys. Rev. A* **2013**, *88*, 043610. [CrossRef]
71. McGuinness, H.J.; Rakholia, A.V.; Biedermann, G.W. High data-rate atom interferometer for measuring acceleration. *Appl. Phys. Lett.* **2012**, *100*, 011106. [CrossRef]
72. Liu, Y.X.; Kan, B.X.; Shi, M.; Wei, X.G.; Wang, X.F. Research progress of atomic gyroscope technology. In Proceedings of the 4th Aerospace Electronics Strategic Research Forum, Beijing, China, 15 June 2018.
73. Fang, B.; Dutta, I.; Gillot, P.; Savoie, D.; Lautier, J.; Cheng, B.; Alzar, C.G.; Geiger, R.; Merlet, S.; Dos Santos, F.P.; et al. Metrology with Atom Interferometry: Inertial Sensors from Laboratory to Field Applications. *Phys. Conf. Ser.* **2016**, *723*, 012049. [CrossRef]
74. Weng, K.X.; Wu, B.; Lin, J.H.; Zhou, Y.; Cheng, B.; Lin, Q. Compact magneto-optical trap with a quartz vacuum chamber for miniature gravimeters. *JOSA B* **2020**, *37*, 1637–1642. [CrossRef]
75. Bharadwaj, K.; Sarkar, S.; Ram, S.P.; Tiwari, V.B.; Mishra, S.R. A compact setup for loading magneto-optical trap in ultrahigh vacuum environment. *arXiv* **2022**, arXiv:2206.13271.
76. McGehee, W.R.; Zhu, W.; Barker, D.S.; Westly, D.; Yulaev, A.; Klimov, N.; Agrawal, A.; Eckel, S.; Aksyuk, V.; McClelland, J.J. Magneto-optical trapping using planar optics. *New J. Phys.* **2021**, *23*, 013021. [CrossRef]
77. Wu, X.; Zi, F.; Dudley, J.; Bilotta, R.J.; Canoza, P.; Müller, H. Multiaxis atom interferometry with a single diode laser and a pyramidal magneto-optical trap. *Optica* **2017**, *4*, 1545–1551. [CrossRef]
78. Earl, L.; Vovrosh, J.; Wright, M.; Roberts, D.; Winch, J.; Perea-Ortiz, M.; Lamb, A.; Hayati, F.; Griffin, P.; Metje, N.; et al. Demonstration of a Compact Magneto-Optical Trap on an Unstaffed Aerial Vehicle. *Atoms* **2022**, *10*, 32. [CrossRef]
79. Zhang, X.; Wang, Y.N.; Li, Q.X.; Zhu, L.X.; Sun, Y.; Jia, A.A.; Zhang, H.K.; Lv, M.J.; Yan, S.H.; Yang, J. Influence of cooling lights' low-frequency pointing instability on the quality of magneto-optical trapping. *J. Opt. Soc. Am. B* **2019**, *36*, 3531–3537. [CrossRef]
80. Jiang, K.J.; Li, K.; Wang, J.; Zhan, M.S. Dependence of number of trapped atoms on the experimental parameters of Rb magneto-optical trap. *Acta Phys. Sin.* **2006**, *55*, 125–129. [CrossRef]
81. Wu, L.M. Optimization of magneto-optical trap parameters based on miniaturized ultra-high vacuum cavity. Master's Dissertation, Zhejiang University of Technology, Hangzhou, China, 2020.
82. Tranter, A.D.; Slatyer, H.J.; Hush, M.R.; Leung, A.C.; Everett, J.L.; Paul, K.V.; Vernaz-Gris, P.; Lam, P.K.; Buchler, B.C.; Campbell, G.T. Multiparameter optimisation of a magneto-optical trap using deep learning. *Nat. Commun.* **2018**, *9*, 4360. [CrossRef]
83. Liu, Q.; Xie, Y.; Li, L.; Liang, A.A.; Li, W.W.; Chen, H.N.; Fang, S.; Qu, Q.Z.; Liu, L.; Wang, B.; et al. Multiparameter Autonomous Optimization System for Ultracold Atomic Experiments Based on Artificial Neural Network. *Chin. J. Lasers* **2021**, *48*, 182–189.
84. Xu, S.; Kaebert, P.; Stepanova, M.; Poll, T.; Siercke, M.; Ospelkaus, S. Maximizing the capture velocity of molecular magneto-optical traps with Bayesian optimization. *New J. Phys.* **2021**, *23*, 063062. [CrossRef]
85. Li, J.X.; Chen, H.J.; Feng, J.J.; Wu, Q.H. Numerical simulation and parameter optimization of novel atomic clock magneto-optical trap for offshore buoys. *J. Shanghai Marit. Univ.* **2023**, *44*, 24–29.
86. Chen, L.; Duan, J.Y.; Yu, Z.L.; Guo, S.; Liu, X.C. Multi parameter autonomous optimization system of mgneto-optical trap based on Bayesian optimization. *Navig. Position Timing* **2023**, *10*, 29–38.
87. Snoek, J.; Larochelle, H.; Adams, R.P. Practical Bayesian Optimization of Machine Learning Algorithms. *Adv. Neural Inf. Process. Syst.* **2012**, *25*, 1–9.
88. Geisel, I.; Cordes, K.; Mahnke, J.; Jöllenbeck, S.; Ostermann, J.; Arlt, J.; Ertmer, W.; Klempt, C. Evolutionary optimization of an experimental apparatus. *Appl. Phys. Lett.* **2013**, *102*, 214105. [CrossRef]
89. Eckel, S.; Barker, D.S.; Norrgard, E.B.; Scherschligt, J. PyLCP: A Python package for computing laser cooling physics. *Comput. Phys. Commun.* **2022**, *270*, 108166. [CrossRef] [PubMed]
90. Hanley, R.K.; Huillery, P.; Keegan, N.C.; Bounds, A.D.; Boddy, D.; Faoro, R.; Jones, M.P. Quantitative simulation of a magneto-optical trap operating near the photon recoil limit. *J. Mod. Opt.* **2018**, *65*, 667–676. [CrossRef]
91. Chen, X.; Zeuner, M.; Schneider, U.; Foot, C.J.; Harte, T.L.; Bentine, E. AtomECS: Simulate laser cooling and magneto-optical traps. *arXiv* **2021**, arXiv:2105.06447.